J Solution Chem (2014) 43:326–339
DOI 10.1007/s10953-014-0129-8

Trace Amounts of Aqueous Copper(II) Chloride Complexes in Hypersaline Solutions: Spectrophotometric and Thermodynamic Studies

Ning Zhang · Quanbao Zhou · Xia Yin · Dewen Zeng

Received: 29 July 2013 / Accepted: 12 October 2013 / Published online: 30 January 2014

Abstract Knowledge of the thermodynamic properties of aqueous copper(II) chloride complexes is important for understanding and quantitatively modeling trace copper behavior in hydrometallurgical extraction processing. In this paper, UV–Vis spectra data of Cu(II) chloride solutions with various salinities (NaCl, 0–5.57 mol·kg^{-1}) are collected at 25 °C. The concentration distribution of Cu–Cl species is in good agreement with those calculated by a reaction model (RM). The simple hydrated ion, Cu^{2+}, is dominant at low concentration, whereas $[CuCl]^{+}$, $[CuCl_2]^{0}$ and $[CuCl_3]^{-}$ become increasingly important as the chloride concentration rises. Moreover, the RM calculation suggests the present of a small amount of $[CuCl_4]^{2-}$. The de-convoluted molar spectrum of each species is in excellent agreement with our previous theoretical results predicted by time-dependent density functional theory treatment of aqueous Cu-containing systems. The formation constants for these copper chloride complexes have been reported and are to be preferred, except $\log_{10} K_2$ ($[CuCl_2]^{0}$).

Keywords Copper(II) species · Copper(II) chloride · UV–Vis spectroscopy

Electronic supplementary material The online version of this article (doi:10.1007/s10953-014-0129-8) contains supplementary material, which is available to authorized users.

N. Zhang · D. Zeng (✉)
College of Chemistry and Chemical Engineering, Central South University, Changsha 410083, People's Republic of China
e-mail: dewen_zeng@hotmail.com

N. Zhang
e-mail: ningcheung@hotmail.com

Q. Zhou
School of Chemistry and Life Science, Guizhou Normal College, Guiyang 550018, People's Republic of China

X. Yin
College of Chemistry and Chemical Engineering, Hunan University, Changsha 410082, People's Republic of China

1 Introduction

The chemical speciation of copper(II) in chloride solutions continues to attract attention, especially because of its relevance to various geochemical [1, 2] and environmental [3] situations. Copper(II)–chloride complexes are also important in the hydrometallurgical extraction of nickel and cobalt, where removal of copper impurities by resin adsorption from chloride-type electrolytes is known to be easier than from sulfate-type ones [4]. According to the National Standard of China (GB/T 6516-1997 Ni9996), the Cu content in nickel electrolysis anolytes should be reduced to <0.01 % ($\sim 5 \times 10^{-4}$ mol·kg^{-1} in the nickel electrolyte) [5] before nickel electro-refining, which is a necessary procedure in order to obtain high-purity nickel. However, it is difficult to separate copper from nickel solution with chloride concentrations higher than 70 g·L^{-1} (~ 2 mol·kg^{-1}) due to certain similar chemical properties [6]. Copper(II) chloride solubility and data for complex formation are required to model chemical behavior in such solutions.

A large number of studies have been devoted to the speciation of Cu(II) in chloride-bearing aqueous brines at room temperature, using methods such as mineral solubility [7], calorimetry [8], and UV–Vis–NIR spectroscopy [1, 9–14]. However, most of these studies were intended to understand the transport and deposition of copper in ore-forming systems [1, 15, 16] and are restricted to one electrolyte and one ionic strength, which does not provide quantitative thermodynamic analysis for the Cu(II) complexes. Bjerrum and co-workers [11–13] investigated Cu(II) speciation of copper chloride in solutions containing other chlorides like those of lithium or calcium by UV–Vis spectroscopy and the results showed that $[CuCl_4]^{2-}$ was absent in the pure $CuCl_2$ solution but was present in a concentrated LiCl solution (7 mol·L^{-1}). Furthermore, the stability constants of copper(II) chloride complexes in HCl up to high chlorinities (12 mol·L^{-1} HCl) were also studied by the same method [14], but his assumption that the tetrachlorocomplex is the only complex absorbing at 436 nm is not strictly valid. Scholz et al. [17] have found the hexahydrated copper ion and tetrachlorocomplex to be present in concentrated copper-containing LiCl solution (1 and 10 mol·L^{-1}) by electronic spectroscopy. A notable exception is the UV–Vis–NIR study (25–90 °C, 1 bar) described in the literature [1], which reports thermodynamic properties for Cu(II) chlorocomplexes and concludes that $[CuCl]^{+}$, $[CuCl_2]^{0}$, $[CuCl]^{3-}$ and $[CuCl_4]^{2-}$ stepwise complexes are the dominant species with increasing Cl^{-} concentration, with the possible presence of $[CuCl_5]^{3-}$ at high salt concentrations (experiments conducted up to 18 mol·kg^{-1} Cl_{tot}).

In this paper, we report the results of a UV–Vis spectroscopic study of the speciation of copper in 0–5.57 mol·kg^{-1} sodium chloride solutions at room temperatures. These measurements are part of a broader project involving the study of complexation reactions in concentrated $NiCl_2$ solution up to 5 mol·kg^{-1}, and Cu(II) concentrations up to the solubility limit. The experimental information will be used to identify the principal species controlling copper behavior in chloride-bearing electrolysis anolytes and to determine their formation constants. NaCl was chosen as the source of chloride because of its available reliable experimental isopiestic data and thermodynamic model [18] over its whole concentration range.

2 Experimental

2.1 Chemicals and Experimental Method

All chemicals except HCl were prepared by doubly crystallizing [19] their respective analytical reagents ($CuCl_2 \cdot 2H_2O$(s), Sinoreagent, China, AR; NaCl(s), Sinoreagent, China,

AR). One set of solutions (NaCl–$CuCl_2$–H_2O system) with the same copper concentration ($\sim 5 \times 10^{-4}$ mol·kg^{-1}) was prepared by mixing (by weight for accuracy) two stock solutions, which were prepared gravimetrically with the same concentration of copper ($CuCl_2 \cdot 2H_2O$(s)), with 0 and 5.57 mol·kg^{-1} NaCl, respectively. A small excess of hydrochloric acid (HCl(aq), Sinoreagent, China, GR) was used to prevent the precipitation of hydroxides. Triple distilled water was used in this work.

Spectrophotometric measurements were made at 1.0 nm intervals over the range 200–500 nm using a Shimadzu (Japan) UV-2550 double-beam spectrophotometer at 25 °C. The dual-beam mode was used where the reference cell contained the same electrolyte solution as the sample cell but without the copper. To correct the spectra for background absorption, the absorption of the cell filled with triple deionized water was recorded before the Cu spectrum was collected. An estimate of the precision of the measurements was obtained by repeated recording (5 scans) of the spectra of solutions having a total copper concentration of $\sim 5 \times 10^{-4}$ mol·kg^{-1} with 0 and 5.57 mol·kg^{-1} NaCl, respectively. It was found that the analytical uncertainty of the spectrophotometer was about 0.003 absorbance units, i.e., 0.3 % for an absorbance of 1.

2.2 Analysis of Spectroscopic Data

In accordance with Beer's law, and assuming a conventional linear model with respect to multiple chemical absorbing species, each of the experimental measurements at any given wavelength can be written as:

$$\frac{A}{l} = \sum_i \varepsilon_i \cdot M_i \tag{1}$$

where A is the absorbance, ε_i is the molar absorptivity coefficient of the corresponding species i, l is the optical path length, and M_i is the molar concentration of the corresponding species i. The molarity scale used in Beer's law was converted to a molality scale for analyzing speciation by a correction factor, $f(\rho)$, being introduced [20] in Eq. 1:

$$\tilde{A} = \frac{A \cdot f(\rho)}{l} = \sum_i \varepsilon_i \cdot m_i \tag{2}$$

with

$$f(\rho) = \frac{1000 + m_{\text{salt}} \cdot W_{\text{salt}}}{1000 \cdot \rho_{\text{salt}}} \tag{3}$$

where m_i is the molality of complex i in the solution, W_{salt} is the molecular mass of NaCl, and ρ_{salt} is the density of NaCl solutions that were calculated using a power series equation [21]. The effect of other solutes on the density of the solutions is neglected in Eq. 3, which is an acceptable approximation for our NaCl dominated systems. Given the correct speciation and an appropriate activity model, it is possible to derive formation constants for the absorbing species by reproducing the measured spectrum, $\tilde{A}$, through optimization of m_i and ε_i. The details are described in the following sections.

2.3 Theoretical Calculations

In order to compare with the experimental result simultaneously, a calculation was also carried out using a reaction model (RM) based on the Stokes–Robinson stepwise hydration

model that was developed [22] to obtain the abundance of each species (see Fig. 6) by the specific Gibbs energies of formation related to the assumed master species.

3 Results

The baseline-corrected spectra for solutions with systematically increasing Cl^- concentrations obtained at room temperature are presented in Fig. 1. For this system, a series of 15 solutions with $\sim 5 \times 10^{-4}$ mol·kg^{-1} $CuCl_2$ were measured spectroscopically. The absorbance band in the range of 230–320 nm shows a systematic redshift with increasing chloride concentration, and the spectrum shows only a weak absorbance in the far UV region at the lowest chloride concentration. As the chloride concentration increases, a band develops at $\sim$250 nm and subsequently increases rapidly in intensity and is redshifted by $\sim$255 and 265 nm in NaCl solutions, respectively. Simultaneously, a new absorption band appears at $\sim$385 nm and another band as a weak shoulder is found at $\sim$243 nm in this system, suggesting that a minimum of four complexes is necessary to interpret the spectra.

3.1 Qualitative Analysis

3.1.1 Speciation Model

Before we can proceed to refine the formation constants, it is necessary to analyze the absorbance matrix for the number of absorbing species. This number was estimated using

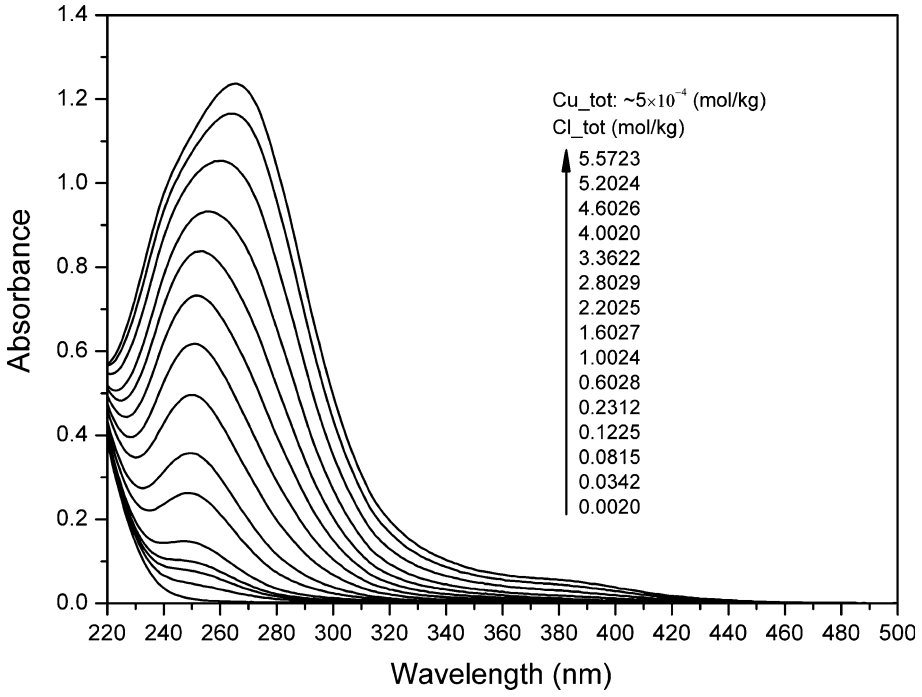

Fig. 1 UV–Visible spectra for the $CuCl_2$–NaCl–H_2O system at 25 °C; the chloride concentration ranged from 0.002 to 5.57 mol·kg^{-1}

principal component analysis (PCA) [23], as in a number of pervious spectroscopic studies [1, 24]. For an accurate analysis result, the absorbance matrix was reduced to restrict it to the wavelength ranges for which peaks are detected (230–500 nm). The results are shown in Fig. 2.

The result of PCA of the spectra collected at room temperature indicates that at least four factors are needed to describe the spectra. It is unlikely that there are more than four complexes contributing to the UV–Vis spectrum, as the calculated residuals for higher factor models are less than the analytical precision and do not decrease markedly between five, six, seven and eight factor models (e.g., the change of slope in Fig. 2). Previous studies have confirmed that the change of spectra as a function of chloride concentration, corresponding to *d–d* electronic transitions at the Cu(II) center [25], is due to the successive replacement of the water ligands with weaker field chloride ligands [1, 19]. Although all of the solutions contained Na^+, H^+ and Cl^-, these species were ignored as they are transparent in the spectral region investigated [26, 27]. Under the chosen experimental conditions, only mononuclear complexes are considered. In view of this and a rank analysis predicting four Cu(II) species, the spectra are attributed to Cu^{2+}, $[CuCl]^+$, $[CuCl_2]^0$ and $[CuCl_3]^-$ and were fitted using these species. In addition to the copper species, Na^+, Cl^-, $[NaCl]^0$ [28], H^+ and $[HCl]^0$ were included in the speciation model for calculating their equilibrium concentrations.

The dissociation constants for $[NaCl]^0$ and $[HCl]^0$, 0.78 and 0.711, were calculated from the thermodynamic properties reported in a literature database [29] and those determined experimentally in the literature [30], respectively.

In the RM calculations to represent the system, the Na^+ ion was assumed to be simply hydrated by a chain of hydration steps $[Na(H_2O)_i]^+$ ($i = 1, 2, 3, 4$) and copper(II)

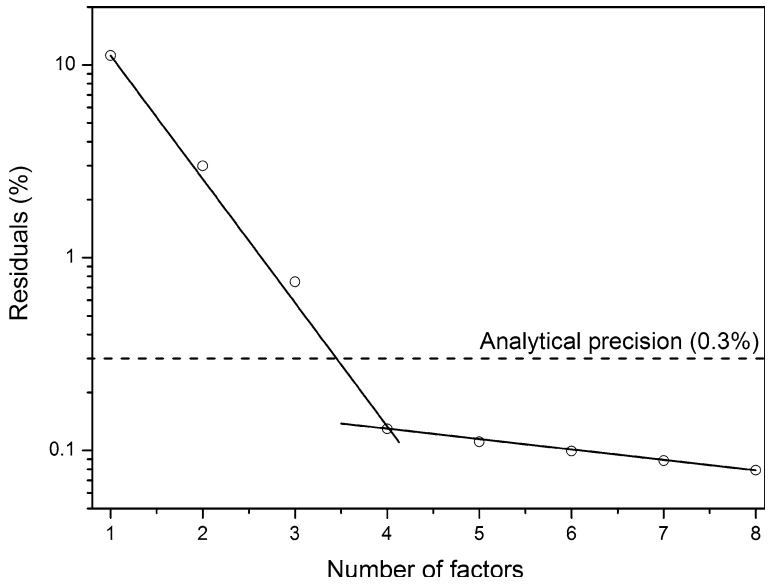

Fig. 2 Results of principal component analysis of the baseline corrected absorption spectra for Cu–Cl solutions at 25 °C. The *circle* represent calculated residuals using $100 \times \sqrt{\frac{(x^{calc} - x^{meas})^2}{x^{calc}}}$, where x^{meas} and x^{calc} stand for the measured and calculated values, respectively. The estimated analytical uncertainty of 0.3 % is shown as a *dashed line*. The *solid lines* have been drawn manually as a visual aid to illustrate the change of slope

complexes were the same as those reported in the literature [22]. Note that $[CuCl_4]^{2-}$ was also considered in the calculation (see Fig. 6). All the selected species and the relevant parameters for the theoretical calculation are listed in Table 1.

3.1.2 Regression Calculations

Equilibrium constants were calculated for the following reactions:

$$Cu^{2+}_{(aq)} + nCl^{-}_{(aq)} \rightleftharpoons [CuCl_n]^{2-n}_{(aq)} \quad K_n (n = 1, 2, 3) \tag{4}$$

The approach used in this study is the same as those described in the literature [26, 31] except that the equilibrium speciation was calculated using the computer program EQBRM (see Eqs. S1–S8 in supplementary materials for detail) [1, 32]. The relevant equations and regression procedure are summarized below.

In order to calculate the concentrations of the ions of interest, an appropriate activity model has to be employed. Since NaCl is always the dominant electrolyte in our solutions, we assumed that activity coefficients of all our ionic species are the same as for the Na^+ and Cl^- ions and elected to use an extended version of the Debye–Hückel equation, the *b*-dot equation [33]:

$$\log_{10}\gamma_i = -\frac{A_\gamma z_i^2 I^{1/2}}{1 + B_\gamma \mathring{a}_i I^{1/2}} + b_{\gamma,\mathrm{NaCl}} I + \Gamma \tag{5}$$

where A_γ and B_γ are the Debye–Hückel solvent parameters taken from the literature [34]; γ_i, z_i and $\mathring{a}_i$ are individual molal activity coefficient, charge, and the distance of closest approach of an ion *i*, respectively. The $\mathring{a}_i$ parameter was fixed at 5 Å for divalent ions and 4 Å for monovalent ions, except for H^+ and Cu^{2+}, which were given values of 9 and 6 Å, respectively [35]. The effective ionic strength using the molal scale is *I*, Γ is the molarity-to-molality conversion factor, and $b_{\gamma,\mathrm{NaCl}}$ is the extended-term parameter for NaCl [18]. Using existing values for *A*, *B*, $\mathring{a}_i$, and $b_{\gamma,\mathrm{NaCl}}$, the dissociation constant for $[NaCl]^0$ (0.78),

Table 1 Assumed species in electrolyte solutions and their Gibbs energies of formation in RM calculation

Systems	Assumed species	Correlation of standard species Gibbs energy	Parameters ($J \cdot mol^{-1}$)
NaCl–H_2O	$[NaCl]^0$, $[Na(H_2O)_1]^+$, $[Na(H_2O)_2]^+$, $[Na(H_2O)_3]^+$, $[Na(H_2O)_4]^+$, Cl^-, H_2O	$G^0_{NaCl} = p_1$, $G^0_{Na(H_2O)_1^+} = 0$, $G^0_{Cl^-} = 0$, $G^0_{H_2O} = 0$, $G^0_{Na(H_2O)_i^+} = (i-1)p_2 + \frac{(i-1)(i-2)}{2}p_3$	$p_1 = -7143.0$ $p_2 = -7195.7$ $p_3 = 5968.1$
$CuCl_2$–H_2O	$[Cu(H_2O)_6]^{2+}$, $[Cu(H_2O)_7]^{2+}$, $[Cu(H_2O)_8]^{2+}$, $[Cu(H_2O)_9]^{2+}$, $[CuCl(H_2O)_5]^+$, $[CuCl_2(H_2O)_{3+2/3}]^0$, $[CuCl_3(H_2O)_2]^-$, $[CuCl_4]^{2-}$, Cl^-, H_2O	$G^0_{Cu(H_2O)_6^{2+}} = 0$, $G^0_{Cl^-} = 0$, $G^0_{H_2O} = 0$, $G^0_{Cu(H_2O)_i^{2+}} = (i-6)p_1$, $G^0_{CuCl_i(H_2O)^{2-i}_{6-i-i(i-1)/6}} = p_2 + (i-1)p_3 + \frac{(i-1)(i-2)}{2}p_4$	$p_1 = -2584.9$ $p_2 = -24580.86$ $p_3 = -7400.5$ $p_4 = 5113.5$

Those for $CuCl_2$–H_2O system from Zhou et al. [22] and used in this study are also listed

and assuming the activity coefficients of neutral species are equal to one, the *b*-dot equation reproduces the experimental mean stoichiometric activity coefficients of NaCl accurately up to ~ 1 mol·kg^{-1} NaCl. At greater NaCl concentrations, the predicted values are less than the measured values and diverge with increasing NaCl concentration (Fig. 3). To fit the entire range of NaCl concentrations for which experimental data are available, a quadratic term $b_{sq,NaCl}I^2$ is added to extend the *b*-dot equation (Eq. 5) to high chloride concentration solutions [1]:

$$\log_{10}\gamma_i = -\frac{A_\gamma z_i^2 I^{1/2}}{1 + B_\gamma \overset{o}{a}_i I^{1/2}} + b_{\gamma,NaCl} I + b_{sq,NaCl} I^2 + \Gamma \tag{6}$$

For neutral ion pairs ($[NaCl]^0$ and $[CuCl_2]^0$) the activity coefficients were obtained from the following equation [32]:

$$\log_{10}\gamma_n = b_n I + \Gamma \tag{7}$$

where b_n is usually referred to as the Setchénow coefficient for neutral a ion pair *n*. For the neutral molecule $[NaCl]^0$, $b_{\gamma,NaCl}$, $b_{sq,NaCl}$ and b_n were fitted to the mean ionic activity coefficients for NaCl [36] following a published procedure [18, 37] and are (0.0487, 0.00235, and 0.364) at 25 °C. Figure 3 shows that the Eq. 6 accurately reproduces the experimental values of the mean stoichiometric molal activity coefficients of NaCl over the

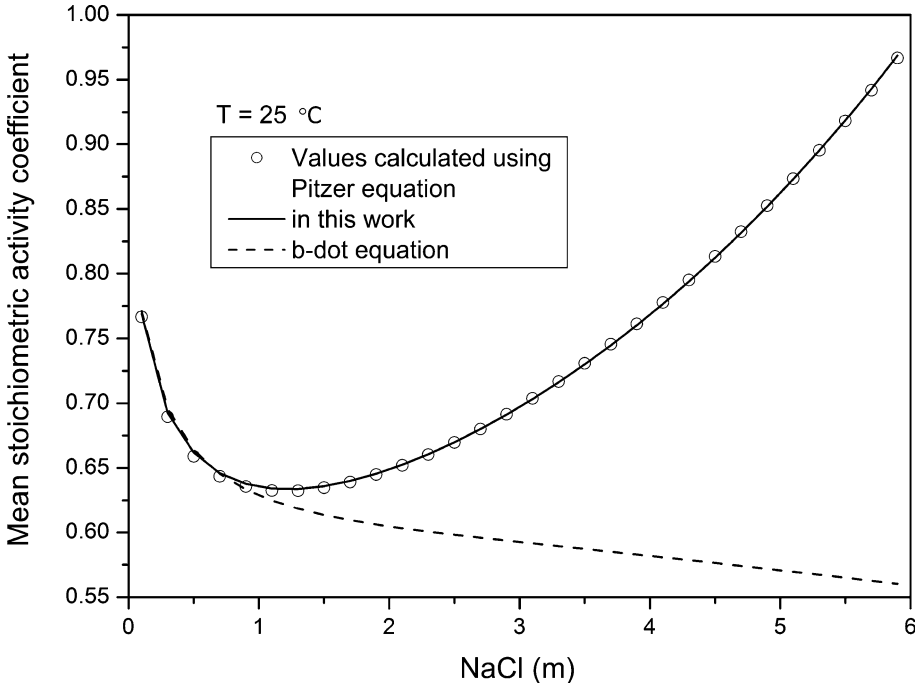

Fig. 3 The mean stoichiometric molal activity coefficients of NaCl solution: the *circles* represent the values calculated using Pitzer parameters from Ref. [36]; The *dashed line* shows predicted values using parameters from Ref. [18] and Eq. 5; the *solid line* shows predicted values using parameters and Eqs. 6 and 7 derived in this study

range of concentrations used in our experiment. The ion pair $[CuCl_2]^0$ was observed by Brugger et al. [1]; assigning the Setchénow coefficient for this species a value in a reasonable interval, $0 < b_n < 0.3$, does not affect appreciably the values of the regressed formation constants for copper–chloride complexes but may change considerably the relative distribution of different complexes. Brugger and co-workers adopted $b_n = 0.1$ for the neutral complex, which is an "intermediate" value leading to molar absorptivity coefficients ε_i in Eq. 1 that are similar in magnitude for all complexes and to a species distribution that does not suppress any of the complexes. We confirmed these observations during the analysis of our data and finally applied the same approach for the activity coefficient of $[CuCl_2]^0$ for the sake of consistency with the pervious literature results. In the case of $[HCl]^0$, we assumed $b_n = 0$ (its activity coefficient is one) because it is only a minor species in our experiments and this is a safe approximation.

Following the method described in the literature [1, 26, 27, 31], the equilibrium constants for the reactions given by Eq. 4 were refined iteratively from initial guesses through minimization of the residual function χ:

$$\chi = \sum_{v=1}^{V} \left[\sum_{j=1}^{J} \left(A_{vj}^{\text{meas}} - A_{vj}^{\text{calc}} \right)^2 \right] \tag{8}$$

where V is the total number of wavelengths at which measurements were made, and J is the number of solutions. A_{vj}^{meas} and A_{vj}^{calc} are the measured and calculated absorbances at wavelength v for solution j, which are a function of the concentration of absorbing species and their molar absorptivity coefficients (see Eq. 2). The calculations involved several cycles of iteration in the minimization (Eq. 8, χ) using an optimization algorithm that is described in the literature [38, 39]. Each of the iterations involved calculation of the equilibrium concentrations of all ions using Eqs. 6 and 7 and the EQBRM program [1, 32]. The concentrations of copper species were used to de-convolute the measured absorbance spectra using a method based on singular value matrix decomposition [40] that was developed for infrared spectra [41] and subsequently applied to UV–Vis spectra (see Eqs. S9–S13 in supplementary materials for details) [26, 31, 42, 43]. At the end of each of the iterations, the values of the molar absorptivity coefficients were used to model spectra of the experimental systems (A_{vj}^{calc}), and to calculate χ until the local minimum for the residual function (Eq. 8) were determined. The optimization procedure is shown in detail as Fig. S1 in the supplementary material.

3.1.3 Results of Fitting

Comparisons of the measured and calculated absorbances are illustrated in Fig. 4 for a cross section at a wavelength of 245, 275 and 350 nm. The values of the optimized formation constants are listed in Table 2. The uncertainties in the derived $\log_{10} K$ values were estimated as described in the literature [26, 31]. Note that stable solutions were not obtained for $\log_{10} K_2$. This is probably because the changes in the spectra approach the experimental uncertainty and the corresponding species is present in low concentrations [44]. The value of $\log_{10} K_2$ (−0.25) shown in Table 2 represents the solutions closest to the value of the literature [29] and is in the range of values of the literature [1] (If the value was much closer to their values, the molar absorptivity coefficients or species distribution would be unreasonable). It is nevertheless considered uncertain and should be used with caution.

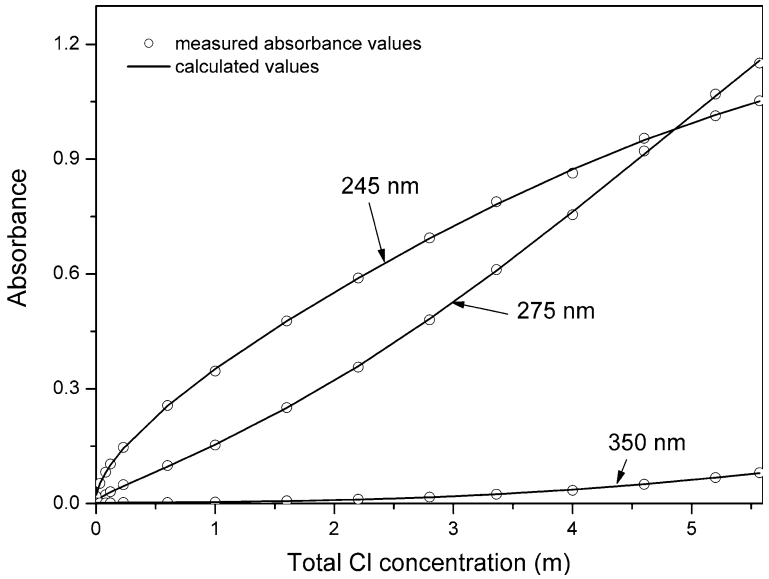

Fig. 4 Comparison of the measured absorbance values (*circles*) and calculated values (*lines*) at 245, 275 and 350 nm for 25 °C

Figure 5 shows the calculated molar absorptivity coefficients of individual complexes, which present a systematic shift to lower energy (redshift) with an increase in the number of chloride ligands. These changes are consistent with the observed redshift in the molar absorbance of the system (Fig. 1). Comparison of the extracted spectra for $[CuCl]^{+}$, $[CuCl_2]^{0}$ and $[CuCl_3]^{-}$ to those of our pervious work [45–47] calculated by time-dependent density functional theory (TD-DFT) reveals excellent agreement of the spectral features (Fig. 5). The calculated distributions of absorbing species are shown in Fig. 6. These are also in good agreement with those predicted by the RM calculation which shows that $[CuCl_4]^{2-}$ should be a minor species in the present study. These observations and comparisons confirm the reliability of the data analysis and the values determined for the formation constants of the aqueous copper chloride complexes.

4 Discussion

In Table 2, we compare our formation constants to those obtained spectroscopically in the literature [1, 14], and those obtained by the theoretical predictions of the literature [29]. As can be seen from Table 2, the value for $\log_{10} K_1$ obtained in the literature [1] is in good agreement with the one derived in this study and is close to the earlier estimates in the literature [29].

The value for $\log_{10} K_3$ differs somewhat from earlier results [1, 29] although those values are within the estimated error. This disagreement is due at least partly to differences in the data sources employed in the calculated activity coefficients (Eqs. 6 and 7 for fitting parameters $b_{\gamma,\mathrm{NaCl}}$ and b_n). The data sources employed in our study are from Pitzer and co-workers [36] which are strictly valid covering the concentration range from 0 to 6 $\mathrm{mol \cdot kg^{-1}}$ for NaCl solution, whereas those of Brugger et al. [1] were obtained by

Table 2 The logarithms of the formation constants ($\log_{10} K$) for copper(II) chloride complexes determined at 25 °C in this study

$\log_{10} K_1$ $[CuCl]^+$	$\log_{10} K_2$ $[CuCl_2]^0$	$\log_{10} K_3$ $[CuCl_3]^-$	Ref.
0.27 (−0.1/+0.2)	−0.63 (−0.1/+0.4)	−2.44 (−0.3/+0.6)	[1]
0.40	−0.69	−2.29	[29]
~0	~0.4	~1.2	[14]
0.241 (−0.1/+0.1)	−0.25[a]	−1.788 (−0.2/+0.5)	This work

Uncertainty limits are given in parentheses

[a] The value cannot be reliably determined (see text)

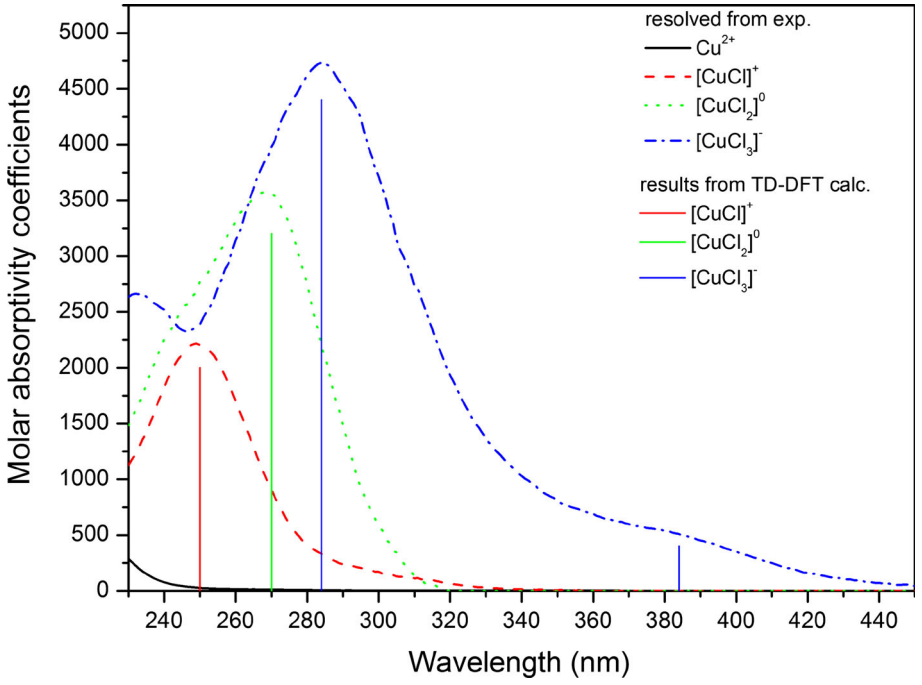

Fig. 5 Molar absorptivity coefficients for copper species (Cu^{2+}, $[CuCl]^+$, $[CuCl_2]^0$ and $[CuCl_3]^-$) at 25 °C obtained from the de-convolution of the experimental spectra in this study (*curved line*) and compared with those calculated using TD-DFT (*line* segment) in the literature [45–47]

extrapolating the LiCl solution concentration to ~19 mol·kg^{-1} from the data of the literature [48] which only had validity over the concentration range from 0 to 6 mol·kg^{-1}. In consequence, at high concentration (>10 mol·kg^{-1} LiCl solution) the extrapolated data are ~10 times higher than those of the literature [49] which were modeled using extremely precise water activity data obtained by the isopiestic measurement method covering concentration range from 0 to 19.8 mol·kg^{-1} for LiCl solution.

By contrast, the values of $\log_{10} K_1$ and $\log_{10} K_3$ in the literature [14] differ by roughly 0.25 and 2.99 $\log_{10}$ units from our experimentally determined value. One reason that may account for this difference is that they assumed only one copper chloride species in

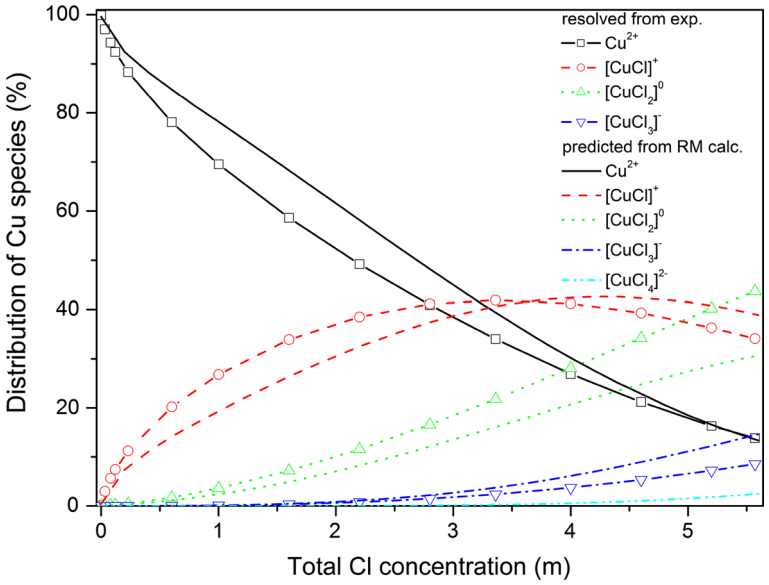

Fig. 6 Proportions of the different copper species in the experimental solutions at 25 °C, calculated using the $\log_{10} K$ values determined in this study (*line* + *symbol*) and using RM (*line*)

solutions at a specific wavelength (e. g., only $[CuCl_4]^{2-}$ present at 436 nm) which is not strictly valid, especially in our case (Cu(II) in chloride-bearing aqueous brines) where spectra for the individual complexes greatly overlap.

The results of speciation calculations using the obtained formation constants show that the Cu^{2+} is the dominant species at low chloride concentrations. With increasing chloride concentration the $[CuCl]^{+}$, neutral and negative chloride complexes become increasingly important. There is even the presence of minor amounts of the quadricovalent copper complex at $\sim$5.5 mol·kg^{-1} Cl_{tot} by our RM calculation. Compared to Ni(II), the result of quantitative X-ray absorption spectroscopy (XAS) refinements [50] is that only 0.9 ($\pm$0.5) Cl^{-} is bonded to Ni(II) at 7.2 mol·kg^{-1} Cl_{tot} (trace amounts of $NiCl_2$ in LiCl solution, $Cl^{-}/Ni^{2+} > 2$) under ambient conditions. Considering the stoichiometric concentrated solutions of $NiCl_2$ ($Cl^{-}/Ni^{2+} = 2$), however, a recent investigation of DFT calculation, Car–Parrinello molecular dynamics (CPMD) simulations and extended X-ray absorption fine structure (EXAFS) spectra [51] gives an explicit picture that there is no obvious evidence for Ni–Cl contact ion pairs even in the saturated aqueous $NiCl_2$ solution (5.05 mol·kg^{-1}). All of this information indicates that Cu(II)–chloride complexes are abundantly presence (in high chloride concentration) and are more easily formed than nickel(II)–chloride complexes in nickel electrolysis anolytes. Further studies need to be done to reveal the cause of the different behavior of Cu and Ni complexes.

5 Conclusions

The UV–Vis spectra of Cu-bearing aqueous solutions were measured at 25 °C in acidic solutions containing between 0 and 5.57 mol·kg^{-1} NaCl. The spectra showed a systematic

redshift with increasing chloride concentration. Chloride-bearing aqueous solutions of copper contain at least four Cu(II) species: Cu^{2+}, $[CuCl]^{+}$, $[CuCl_2]^{0}$ and $[CuCl_3]^{-}$. Thermodynamic formation constants of the copper–chloride complexes were retrieved from the experimental data using appropriate physico-chemical constraints. The value of the first formation constants is in near perfect agreement with those of previous estimates, but is higher than this for our third formation constant, indicating that the copper chloride complexes are less stable than previous studies suggest.

At 25 °C and low chloride concentrations, Cu^{2+} is the dominant form of copper(II) in aqueous solutions, and chloride species ($[CuCl]^{+}$, $[CuCl_2]^{0}$ and $[CuCl_3]^{-}$) become increasingly important as the chloride concentration rises. Also, the RM calculations show that $[CuCl_4]^{2-}$ is a minor species, which means that processing of the experimental data is reasonable using four species only. Furthermore, an alternative modeling of activity coefficients has been developed, in order to obtain reliable thermodynamic representation of copper chloride complexation suitable for parameterizing engineering models for copper–chloride thermochemical hydrometallurgical extraction processing.

Acknowledgments This research was financially supported by the National Natural Science Foundation of China (Nos. 51134007, 2077306) and the China Scholarship Council (No. 201306370118).

References

1. Brugger, J., McPhail, D.C., Black, J., Spiccia, L.: Complexation of metal ions in brines: application of electronic spectroscopy in the study of the Cu(II)–LiCl–H2O system between 25 and 90 °C. Geochim. Cosmochim. Acta **65**, 2691–2708 (2001)
2. Gunton, C.: The role of salinity on the formation of geochemical anomalies in the regolith. In: Roach, I.C. (ed.) Advances in Regolith: Proceedings of the CRC LEME Regional Regolith Symposia, pp. 154–158, CRC LEME, West Australia (2003)
3. Powell, K.J., Brown, P.L., Byrne, R.H., Gajda, T., Hefter, G.T., Sjöberg, S., Wanner, H.: Chemical speciation of environmentally significant metals with inorganic ligands Part 2: The Cu^{2+}–OH^{-}, Cl^{-}, CO_3^{2-}, SO_4^{2-}, and PO_4^{3-} systems. Pure Appl. Chem. **79**, 895–950 (2007)
4. Wen, J.J.: The fundamental research on removing copper from cobalt electrolyte and nickel electrolyte by ion-exchange with novel silica–polyamine organic–inorganic composite resin. Dissertation, Central South University, Changsha, China (2010)
5. Chen, X.Y., Chen, A.L., Zhao, Z.W., Liu, X.H., Shi, Y.C., Wang, D.Z.: Removal of Cu from the nickel electrolysis anolyte using nickel thiocarbonate. Hydrometallurgy **133**, 106–110 (2013)
6. Lee, C.I., Yang, W.F., Hsieh, C.I.: Removal of copper(II) by manganese-coated sand in a liquid fluidized-bed reactor. J. Hazard. Mater. **114**, 45–51 (2004)
7. Ramette, R.W.: Copper(II) chloride complex equilibrium constants. Inorg. Chem. **22**, 3323–3326 (1983)
8. Arnek, R., Puigdomenech, I., Valiente, M.: A calorimetric study of copper(II) chloride complexes in aqueous solution. Acta Chem. Scand. A **36**, 15–19 (1982)
9. Byrne, R.H., Van der Weijden, C., Kester, D.R., Zuehlke, R.W.: Evaluation of the $CuCl^{+}$ stability constant and molar absorptivity in aqueous media. J. Solution Chem. **12**, 581–596 (1983)
10. Moeller, T.: An application of the method of continuous variations to complexion formation in copper(II) salt solutions containing chloride ion. J. Phys. Chem. **48**, 111–119 (1944)
11. Bjerrum, J.: Optical investigations on cupric chloride in mixtures with other chlorides. Mat.-Fys. Medd.-K. Dan Vidensk. Selsk, vol. 22, pp. 1–43 (1946)
12. Bjerrum, J., Skibsted, L.H.: A contribution to our knowledge of weak chloro complex formation by copper(II) in aqueous chloride solutions. Acta Chem. Scand. A **31**, 673–677 (1977)
13. Bjerrum, J., Skibsted, L.H.: Weak chloro complex formation by copper(II) in aqueous chloride solutions. Inorg. Chem. **25**, 2479–2481 (1986)
14. Bjerrum, J.: Determination of small stability constants. A spectrophotometric study of copper(II) chloride complexes in hydrochloric acid. Acta Chem. Scand. A **41**, 328–334 (1987)
15. Lundstrom, M., Aromaa, J., Forsen, O., Hyvarinen, O., Barker, M.H.: Leaching of chalcopyrite in cupric chloride solution. Hydrometallurgy **77**, 89–95 (2005)

16. Hyvarinen, O., Hamalainen, M.: HydroCopper^{TM}—a new technology producing copper directly from concentrate. Hydrometallurgy **77**, 61–65 (2005)
17. Sholz, H., Ludeman, H.D., Franck, E.U.: Spetra of Cu(II)-complexes in aqueous solutions at high temperatures and pressures. Ber. Bunsenges. Phys. Chem. **76**, 406–409 (1972)
18. Helgeson, H.C., Kirkham, D.H., Flowers, G.C.: Theoretical prediction of the thermodynamic behavior of aqueous electrolytes at high pressures and temperatures: IV. Calculation of activity coefficients, osmotic coefficients, and apparent molal and standard and relative partial molal properties to 600 °C and 5 kb. Am. J. Sci. **281**, 1249–1516 (1981)
19. Shriver, D.F., Atkins, P.W., Langford, H.C.: Inorganic Chemistry, 3rd edn. Oxford University Press, Oxford (1996)
20. Heinrich, C.A., Seward, T.M.: A spectrophotometric study of aqueous iron(II) chloride complexing from 25 to 200 °C. Geochim. Cosmochim. Acta **54**, 2207–2221 (1990)
21. Otakar, S., Petr, N.: Densities of aqueous solutions of inorganic substances. Elsevier, New York (1985)
22. Zhou, Q.B., Zeng, D., Voigt, W.: Thermodynamic modeling of salt–water systems up to saturation concentrations based on solute speciation: $CuCl_2$–MCl_n–H_2O at 298 K (M = Li, Mg, Ca). Fluid Phase Equilib. **322–323**, 30–40 (2012)
23. Malinowski, E.R.: Determination of the number of factors and the experimental error in a data matrix. Anal. Chem. **49**, 612–616 (1977)
24. Liu, W., Brugger, J., Mcphail, D.C., Spiccia, L.: A spectrophotometric study of aqueous copper(II)–chloride complexes in LiCl solutions between 100 °C and 250 °C. Geochim. Cosmochim. Acta **66**, 3615–3633 (2002)
25. Hatfield, W.E., Bedon, H.D., Horner, S.M.: Molecular orbital theory for the pentachlorocuprate(II) ion. Inorg. Chem. **4**, 1181–1184 (1965)
26. Migdisov, A.A., Williams-Jones, A.E., Normand, C., Wood, S.A.: A spectrophotometric study of samarium(III) speciation in chloride solutions at elevated temperatures. Geochim. Cosmochim. Acta **72**, 1611–1625 (2008)
27. Suleimenov, O.M., Seward, T.M.: Spectrophotometric measurements of metal complex formation at high temperatures: the stability of Mn(II) chloride species. Chem. Geol. **167**, 177–192 (2000)
28. Uchida, H., Matsuoka, M.: Molecular dynamics simulation of solution structure and dynamics of aqueous sodium chloride solutions from dilute to supersaturated concentration. Fluid Phase Equilib. **219**, 49–54 (2004)
29. Sverjensky, D.A., Shock, E.L., Helgeson, H.C.: Prediction of the thermodynamic properties of aqueous metal complexes to 1000 C and 5 kb. Geochim. Cosmochim. Acta **61**, 1359–1412 (1997)
30. Tagirov, B.R., Zotov, A.V., Akinfiev, N.N.: Experimental study of dissociation of HCl from 350 to 500 °C and from 500 to 2500 bars: thermodynamic properties of HCl0(aq). Geochim. Cosmochim. Acta **61**, 4267–4280 (1997)
31. Migdisov, A.A., Reukov, V.V., Williams-Jones, A.E.: A spectrophotometric study of neodymium(III) complexation in sulfate solutions at elevated temperatures. Geochim. Cosmochim. Acta **70**, 983–992 (2006)
32. Anderson, G.M., Crerar, D.A.: Thermodynamics in Geochemistry: The Equilibrium Model. Oxford University Press, New York (1993)
33. Helgeson, H.C.: Thermodynamics of hydrothermal systems at elevated temperatures and pressures. Am. J. Sci. **267**, 729–804 (1969)
34. Helgeson, H.C., Kirkham, D.H.: Theoretical prediction of the thermodynamic behavior of aqueous electrolytes at high pressures and temperatures: II. Debye–Hückel parameters for activity coefficients and relative partial molal properties. Am. J. Sci. **174**, 1199–1261 (1974)
35. Kielland, J.: Individual activity coefficients of ions in aqueous solutions. J. Am. Chem. Soc. **59**, 1675–1678 (1937)
36. Pitzer, K.S., Mayorga, G.: Thermodynamics of electrolytes. II. Activity and osmotic coefficients for strong electrolytes with one or both ions univalent. J. Phys. Chem. **77**, 2300–2308 (1973)
37. Pokrovskii, V.A., Helgeson, H.C.: Calculation of the standard partial molal thermodynamic properties of KCl0 and activity coefficients of aqueous KCl at temperatures and pressures to 1000 °C and 5 kbar. Geochim. Cosmochim. Acta **61**, 2175–2183 (1997)
38. Nelder, J.A., Mead, R.: A simplex method for function minimization. Comput. J. **7**, 308–313 (1965)
39. Dennis, J.E., Woods, D.J.: Optimization on microcomputers: The Neld–Mead simplex algorithm. In: Wouk, A. (ed.) New Computing Environments: Microcomputers in Large-Scale Computing, pp. 116–122. SIAM, Philadelphia (1987)
40. Golub, G.H., Reinsch, C.: Singular value decomposition and least squares solutions. Numer. Math. **14**, 403–420 (1970)

41. Hug, S.J., Sulzberger, B.: In situ Fourier transform infrared spectroscopic evidence for the formation of several different surface complexes of oxalate on TiO_2 in the aqueous phase. Langmuir **10**, 3587–3597 (1994)
42. Boily, J.F., Seward, T.M.: Palladium(II) chloride complexation: spectrophotometric investigation in aqueous solutions from 5 to 125 °C and theoretical insight into Pd–Cl and Pd–OH_2 interactions. Geochim. Cosmochim. Acta **69**, 3773–3789 (2005)
43. Boily, J.F., Suleimenov, O.M.: Extraction of chemical speciation and molar absorption coefficients with well-posed solutions of Beer's law. J. Solution Chem. **35**, 917–926 (2006)
44. Liu, W., Etschmann, B., Brugger, J., Spiccia, L., Foran, G., Mcinnes, B.: UV–Vis spectrophotometric and XAFS studies of ferric chloride complexes in hyper-saline LiCl solutions at 25–90 °C. Chem. Geol. **231**, 326–349 (2006)
45. Xia, F.F., Yi, H.B., Zeng, D.: Hydrates of copper dichloride in aqueous solution: a density functional theory and polarized continuum model investigation. J. Phys. Chem. A **113**, 14029–14038 (2009)
46. Xia, F.F., Yi, H.B., Zeng, D.: Hydrates of Cu^{2+} and $CuCl^{+}$ in dilute aqueous solution: a density functional theory and polarized continuum model investigation. J. Phys. Chem. A **114**, 8406–8416 (2010)
47. Yi, H.B., Xia, F.F., Zhou, Q.B., Zeng, D.: $[CuCl_3]^{-}$ and $[CuCl_4]^{2-}$ hydrates in concentrated aqueous solution: a density functional theory and ab initio study. J. Phys. Chem. A **115**, 4416–4426 (2011)
48. Holmes, H.F., Mesmer, R.E.: Thermodynamic properties of aqueous solutions of the alkali metal chlorides to 250 °C. J. Phys. Chem. **87**, 1242–1255 (1983)
49. Yao, Y., Sun, B., Song, P.S., Zhang, Z.: Thermodynamics of aqueous electrolyte solutions isopiestic determination of osmotic and activity coefficients in LiCl–$MgCl_2$–H_2O at 25 °C. Acta Chim. Sin. **50**, 839–848 (1992)
50. Tian, Y., Etschmann, B., Liu, W.H., Borg, S., Mei, Y., Testemale, D., O'Neill, B., Rae, N., Sherman, D., Ngothai, Y., Johannessen, B., Glover, C., Brugger, J.: Speciation of nickel(II) chloride complexes in hydrothermal fluids: in situ XAS study. Chem. Geol. **334**, 345–363 (2012)
51. Xia, F.F., Zeng, D., Yi, H., Fang, C.: Direct contact versus solvent-shared ion pairs in saturated $NiCl_2$ aqueous solution: a DFT, CPMD, and EXAFS investigation. J. Phys. Chem. A **117**, 8468–8476 (2013)